

Clinical Evaluation of a Photon-Counting Tomosynthesis Mammography System

Andrew D.A. Maidment¹, Christer Ullberg², Tom Francke², Lars Lindqvist², Skiff Sokolov², Karin Lindman², Leif Adelow², and Per Sunden³

¹ University of Pennsylvania, Department of Radiology,
3400 Spruce Street, Philadelphia, PA USA 19104
andrew.maidment@uphs.upenn.edu

² XCounter AB, Svärdvägen 11, SE - 182 33 Danderyd, Sweden
{christer.ullberg, tom.francke, lars.lindqvist, skiff.sokolov,
karin.lindman, leif.adelow}@xcouter.se

³ Danderyds Sjukhus, Mammography Department,
AB 182 88 Stockholm, Sweden
per.sunden@ds.se

Abstract. Digital breast tomosynthesis promises solutions to many of the problems currently associated with projection mammography, including elimination of artifactual densities from the superposition of normal tissues and increasing the conspicuity of true lesions that would otherwise be masked by superimposed normal tissue. We have investigated the performance of a novel tomosynthesis system in a clinical setup. The novel system uses 48 photon counting, orientation sensitive, linear detectors which are precisely aligned with the focal spot of the x-ray source. The x-ray source and the digital detectors are scanned in a continuous motion across the patient; each linear detector collecting an image at a distinct angle. The results from an assessment of image quality and the initial clinical trial of this device are presented. Initial results provide anecdotal evidence supporting the superiority of tomosynthesis over projection mammography.

1 Background

There are a number of problems currently associated with projection mammography, including decreased conspicuity of true lesions that are masked by superimposed normal tissue and artifactual densities from the superposition of normal tissues [1]. Tomosynthesis is a promising solution to overcome these problems [2-5]. However, tomosynthesis systems based on area flat-panel detectors themselves suffer from a number of fundamental limitations. First, the requirement of sequential image acquisition limits the number of images acquired; acquiring an insufficient number of images results in image artifacts [6, 7]. Second, electronic noise, ghosting and lag found in each of the source projection images are added in the reconstruction process, resulting in excessive noise in the reconstructed images. Third, the long readout time of current flat panel detector technology results in image blurring, both from patient motion, and from the continuous scanning motion used in some systems.

2 Imaging System

A novel tomosynthesis system has been developed [6-10]. The system uses 48 photon-counting, orientation sensitive, linear detectors which are precisely aligned with the focal spot of the x-ray source. The x-ray source and the digital detectors are scanned in a continuous motion across the patient; each linear detector collecting an image at a distinct angle.

The 48 simultaneously collected images are of very high image quality due to several special characteristics of this detector technology. First, the detectors are insensitive to scattered radiation; the detector geometry ensures that only primary photons emanating from the focal spot of the x-ray source will elicit a response from the detector. Second, the detector does not contribute any electronic noise; the strong gaseous amplification of each photon interaction allows a simple threshold to exclude electronic noise from being counted and included in the final image. Third, the image pixels are very small ($60\ \mu\text{m}$) avoiding motion blurring from long scanning times of each sub-image. Finally, the detector technology does not have any residual image, ghosting or blooming artifacts.

Data appropriate for tomosynthesis is acquired over a region $24 \times 30\ \text{cm}^2$ within 15 seconds. The resulting 48 projection images are then reconstructed using filtered back-projection to produce a volumetric data set of tomographic images. The images are presented on a dedicated primary review workstation for interpretation.

The imaging system is typically operated with a tube potential of between 30 and 40 kVp with a W-target anode and Al filtration. The mean glandular dose for a tomosynthesis image is typically less than or equal to a normal film/screen mammogram. The system is shown in Figure 1.



Fig. 1. The imaging system is shown. The system is capable of both projection mammography and tomosynthesis. The system is wider than conventional systems to accommodate the scanning detector and x-ray source.

3 Clinical Trial

Method: An initial clinical study of this novel tomosynthesis system has recently been completed. Enrolment was limited to 20 patients. The study was conducted with IRB oversight. All patients provided informed consent. Patient recruitment was limited to women having clinical and/or mammographic findings; specifically, they either had to be recalled after an abnormal screening mammogram or be referred by a physician after suspicious physical findings.

For each patient, analog film images were first taken at Danderyd Sjukhus (Danderyd, Sweden). Later the same day, digital tomosynthesis images were taken of the same breast by the same radiologic nurse. The digital tomosynthesis images were then reviewed by a trained radiologist.

Dosimetry: Twenty patients were enrolled in the clinical trial. The film-screen radiographs were acquired at either 30 or 31 kVp, with an average entrance skin air kerma (ESAK) of 6.68 ± 4.83 mGy, and average glandular dose (AGD) of 1.46 ± 0.73 mGy. By comparison, the tomosynthesis images were acquired at 30-35 kVp and 140-180 mA, resulting in an average ESAK of 4.98 ± 0.61 mGy, and an AGD of 1.42 ± 0.16 mGy.

Clinical Evaluation: Our initial goal was to seek anecdotal proof that the tomography system provided clinically acceptable breast images. Criteria included breast positioning, resolution of high-contrast structures such as calcifications and clips, and conspicuity of larger low-contrast objects such masses and cysts.

A preliminary analysis indicates that the image quality achieved to date is clinically acceptable. Figure 1 demonstrates the system being used for a medial-lateral oblique (MLO) mammogram. Breast positioning for both MLO and cranio-caudal (CC) mammograms appear to be acceptable [7]. The MLO images, when reconstructed near the mid-plane of the breast, typically show that the pectoralis muscle extends below the line drawn perpendicular to the muscle that passes through the nipple. The CC images typically show the posterior margin of the glandular tissue (for example, see Fig. 2).

The images to date have shown very high spatial resolution. In general, we see more calcifications in the tomosynthesis images than in the screen-film mammograms. Further, the calcifications in the tomosynthesis images are generally better resolved (sharper margins and higher contrast) than in the screen-film images. We find that calcifications rapidly disappear when out-of-plane. These observations are consistent with our previous findings with phantoms and animals, and are likely due to the choice of angular range, number of projection images and pixel size.[6]

The images (see Fig. 2) depict the breast anatomy well. The glandular tissue, adipose tissue, Cooper's ligaments, blood vessels, lymph nodes and other structures of the breast are well visualized. In the 20 women studied we found one cancer which was quite obvious in the tomosynthesis image, and only marginally visible in the screen-film image. While anecdotal, we believe that these early images provide convincing evidence of the superiority of both tomosynthesis and our approach of simultaneously acquiring multiple images with a scanning photon-counting detector. We believe that the system is capable of producing images with clinically acceptable

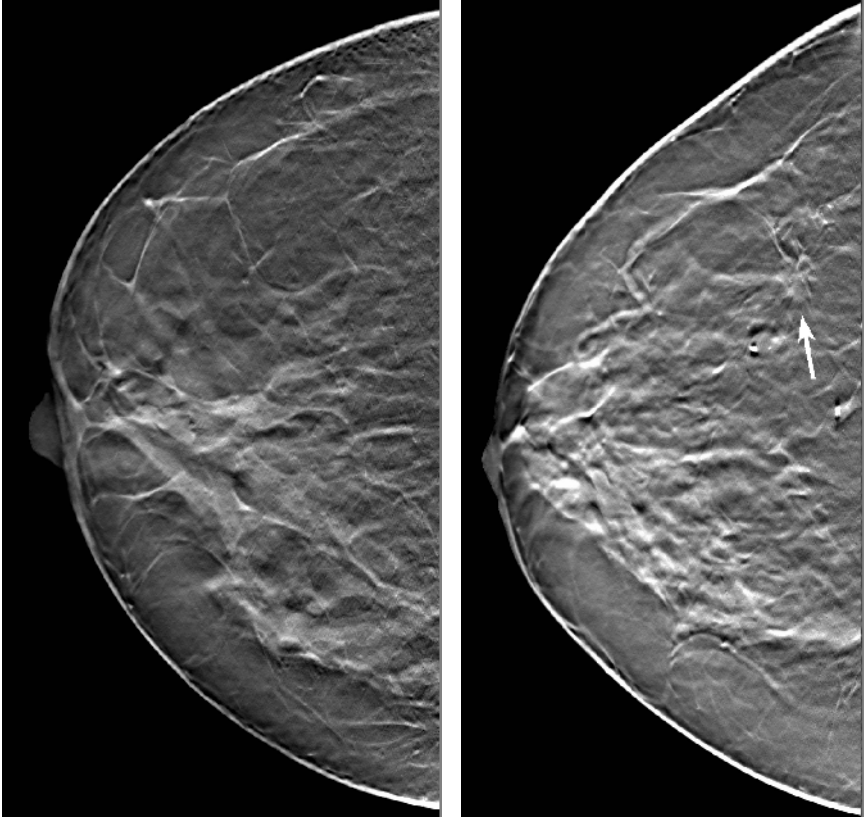


Fig. 2. Reconstructions from 2 patients. The patient on the left has numerous calcifications that are clearly seen. The patient on the right has a spiculated mass, which on biopsy was identified as a ductal carcinoma.

quality, and having adequate tissue penetration and breast positioning. Admittedly, these results are preliminary and lack statistical significance.

4 Assessment of Image Quality

Image quality has been assessed by multiple methods, including the assessment of the modulation transfer function (MTF) and the noise power spectrum (NPS).

MTF: The MTF in the scanning and strip (i.e., parallel to the linear detector strips) directions have been measured. The MTF was measured using a slanted edge method [11]. The edge was measured in an image reconstructed with simple back-projection, in the plane of the edge. Figure 3 shows the measured MTF in the scanning direction. These data are shown compared to theoretical calculations. The theoretical MTF can be decomposed into 2 main sources of blurring. The first is related to scanning unsharpness. The detector is read out each time the detector array

is translated $60\ \mu\text{m}$. Thus, the scanning unsharpness can be represented by a sinc function. The second source of unsharpness is related to the image acquisition geometry; the collimator is at a fixed distance above the breast and the x-ray focal spot is of known size and shape. Thus, it is possible to calculate the blurring due to the collimator width and geometric unsharpness as the product of two sinc functions, assuming that the focal spot has a rectangular intensity profile. The product of these two sources of unsharpness is specified as the “Total” in Figure 3. The similarity of the measured and experimental data is noteworthy. The discrepancy seen is likely due to deviation from the assumption of a rectangular focal spot.

Figure 4 shows the measured MTF in the scan and strip directions. The resolution in the strip direction is lower than that in the scan direction. This degradation is still under investigation; however, it is likely due to simultaneous triggering of adjacent channels in the detector.

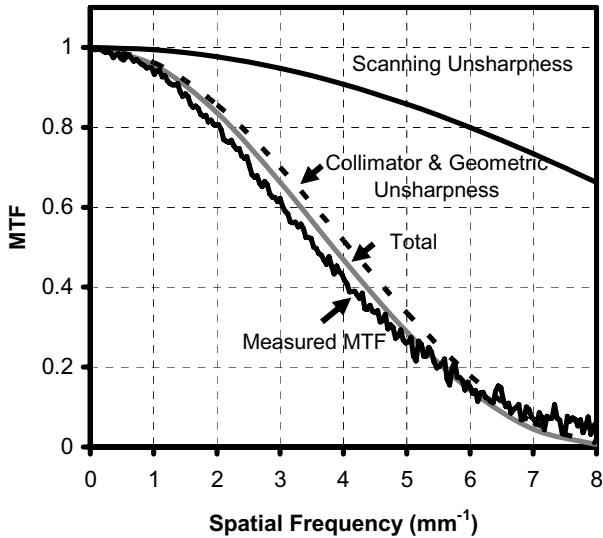


Fig. 3. System MTF of tomographic images in the scanning direction. Both measured and theoretical data are presented. The theoretical unsharpness is divided into two terms: scanning unsharpness, and collimator and geometric unsharpness. Their product is labeled “Total”. The theoretical total MTF is quite similar to the measured MTF.

NPS: Images to calculate the NPS were acquired at 35 kVp with a W-target x-ray tube and 0.5 mm Al filtration. A uniform block of PMMA 40 mm thick was imaged. From these projection images, 128 planes with 0.3 mm separation were reconstructed using both simple backprojection and filtered backprojection. Using these data, a volume of interest (VOI) $38\times 60\times 200\ \text{mm}$ ($128\times 1024\times 3328$ pixels) was selected with the largest dimension parallel to the chest wall. The VOI size and orientation were chosen to minimize the heel effect. A VOI 200 mm long is acceptable due to the scanning geometry. The VOI was then divided into $128\times 128\times 128$ voxel cubes

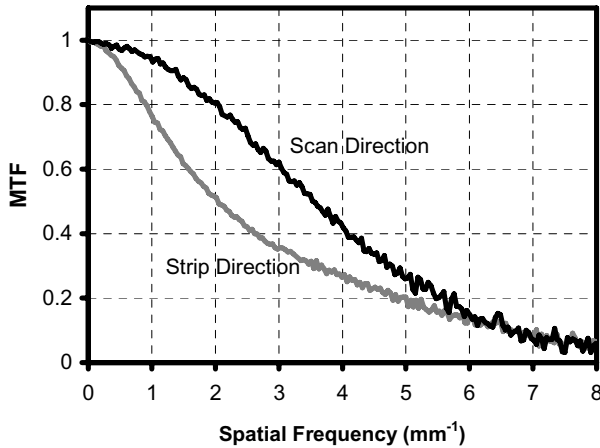


Fig. 4. MTF of tomographic images in the scan and strip directions. The MTF in the strip direction is reduced compared to the scan direction due to simultaneous triggering of adjacent channels.

overlapping by 64 pixels in both the x and y directions. A 3D spectral estimate was calculated for each cube, and these estimates were averaged to calculate the NPS.

The NPS are shown in Fig. 5 for the case of simple (a, c) and filtered (b, d) back-projection, presented logarithmically. The same grayscale is used for the simple and filtered spectra. The axes are labeled with the spatial orientation corresponding to the spatial frequencies shown, where X denotes the direction along the chestwall, Y denotes the orthogonal direction from the chestwall to the nipple, and Z is the direction perpendicular to the detector. The origin is located at the center of the cube.

There are many notable features in the NPS. As shown previously, the NPS of the projection images produced with the system are essentially white [7]. Restated, there is little correlation in the images. This can be seen in Fig. 1a and c, where the NPS can roughly be segmented into areas of white noise (the uniform light gray regions) and no noise (the uniform dark gray regions). This segmentation allows us to define the null space [12] of the imaging system as the latter region. An examination of the null space clearly demonstrates one of the benefits of photon-counting detectors in tomosynthesis, as there is virtually no noise in the regions of space not supported by the angular sampling. The complement to the null space clearly demonstrates which spatial frequencies are supported in the reconstruction.

Comparing Figs. 1a and c to Figs. 1b and d, the effect of the filter is made clear. In the example shown, the filter that was used suppressed high spatial-frequencies in the X-direction. This is consistent with the two large dark bands running vertically in the Z-direction on the lateral sides of the X-Z face (Fig 1b and d). Very low spatial frequencies in the X-direction are also suppressed, as can be seen by the dark vertical band that divides the X-Z face and X-Y face (Fig. 1b).

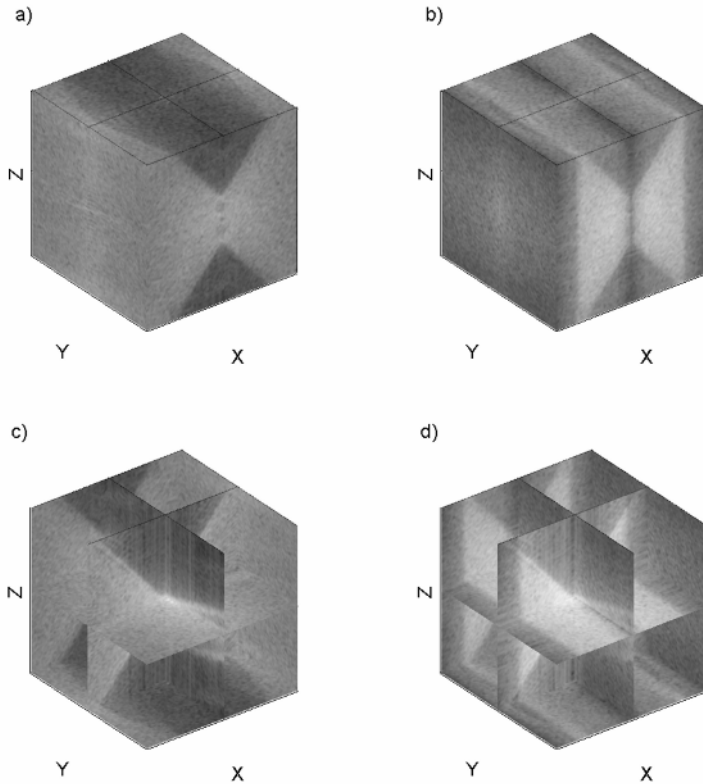


Fig. 5. The logarithm of the NPS is shown in 3D for the case of simple (a, c) and filtered (b, d) back-projection. The axes are labeled with the spatial orientation corresponding to the spatial frequencies shown (X, the direction along the chestwall; Y, the orthogonal direction from the chestwall to the nipple; Z, the direction perpendicular to the detector).

5 Discussion

A novel tomographic imaging system has been developed. The detector technology is the first to have been developed specifically for tomosynthesis imaging. As such, it offers numerous technical advantages over tomosynthesis with flat panel detectors. The first clinical trial of the system is complete. Initial clinical results demonstrate outstanding image quality and diagnostic value. To date, these results are anecdotal. A retrospective reader trial is planned to determine more quantitative measures.

The clinical trial was performed at a dose comparable to screen-film mammography. It is important to realize that the dose in a digital image is somewhat arbitrary, as the system is linear and has very wide dynamic range. However, there are two relevant questions: (1) is the resultant image x-ray quantum noise limited to high spatial-frequency; and (2) are the images of clinical quality. We believe that the NPS analysis establishes the former. We further believe that the outstanding image quality of the clinical images to date provide anecdotal proof of the latter. Thus, it is notable

that the tomosynthesis images were acquired at a lower dose than the screen-film mammograms, yet appear to have comparable or superior image quality.

Acknowledgments

This work is funded in part by NIH grant PO1 CA85484-01.

References

- [1] Ma L, Fishell E, Wright B, *et al.* Case-control study of factors associated with failure to detect breast cancer by mammography. *Journal of the National Cancer Institute* 1992;84(10):781-5.
- [2] Dobbins JT, 3rd, Godfrey DJ. Digital x-ray tomosynthesis: current state of the art and clinical potential. *Physics in Medicine & Biology* 2003;48(19):R65-106.
- [3] Niklason LT, Christian BT, Niklason LE, *et al.* Digital tomosynthesis in breast imaging. *Radiology* 1997;205(2):399-406.
- [4] Rafferty EA. Tomosynthesis: New Weapon in Breast Cancer Fight. *Decisions in Imaging Economics* 2004;17(4).
- [5] Wu T, Moore RH, Rafferty EA, *et al.* Breast tomosynthesis: Methods and applications. In: Karellas A, editor. *RSNA Categorical Course in Diagnostic Radiology Physics: Advances in Breast Imaging - Physics, Technology, and Clinical Applications*; 2004. p. 149-163.
- [6] Maidment ADA, Albert M, Thunberg S, *et al.* Evaluation of a Photon-Counting Breast Tomosynthesis Imaging System. In: Flynn MJ, editor. *SPIE Medical Imaging 2005*; p. 572-82.
- [7] Maidment ADA, Adelow L, Blom O, *et al.* Evaluation of a Photon-Counting Breast Tomosynthesis Imaging System. In: Flynn MJ, editor. *Physics of Medical Imaging, Proc. SPIE 6142*; 2006.
- [8] Thunberg S, *et al.* Evaluation of a Photon Counting Mammography System. In: *SPIE Medical Imaging 2002* p. 202-208.
- [9] Thunberg S, Maidment ADA, *et al.* Dose reduction in Mammography with Photon Counting Imaging. In: *SPIE Medical Imaging 2004*; p. 457-465.
- [10] Thunberg S, Maidment ADA, *et al.* Tomosynthesis with a Multi-line Photon Counting Camera. In: Pisano E, editor. *7th International Workshop on Digital Mammography*; 2004; p. 459-465.
- [11] Kao Y-H, Maidment ADA, Albert M, *et al.* Assessment of a software tool for measurement of the modulation transfer function. In: Flynn MJ, editor. *Medical Imaging 2005: Physics of Medical Imaging*; p. 1199-1208.
- [12] Myers KJ, Barrett HH. *Foundations of Image Science*. New York, NY: John Wiley & Sons; 2004.